Program Digest, 2019 IEEE International Ultrasonics Symposium (IUS)
Glasgow, Scotland, October 6-9, 2019

Detecting Deep Brain Stimulation Currents with High Resolution Transcranial Acoustoelectric Imaging

Chet Preston
Biomedical Engineering
University of Arizona
Tucson, AZ, USA
chetpreston@email.arizona.edu

Alexander Alvarez
Biomedical Engineering
University of Arizona
Tucson, AZ, USA
alexanderalvarez@email.arizona.edu

Andres Barragan
Computer Science
University of Arizona
Tucson, AZ, USA
andresbarragan@email.arizona.edu

Willard S. Kasoff
Surgery
University of Arizona
Tucson, AZ, USA
wkasoff@surgery.arizona.edu

Russell S. Witte
Medical Imaging
University of Arizona
Tucson, AZ, USA
rwitte@email.arizona.edu

Abstract— **The efficacy of deep brain stimulation (DBS) for relieving motor symptoms from Parkinson's disease or essential tremor is highly dependent on accurate placement of the electrode. New current-steering electrodes can reduce the burden of placement by directing the stimulating currents toward the target locations. However, no imaging modality exists in the clinic or operating room to provide feedback of the currents as they are delivered/steered from the contacts. In this study we investigate the prospects of high resolution, transcranial acoustoelectric imaging (AEI) as a method for non-invasively imaging DBS currents. A DBS electrode was inserted into a brain gel phantom inside a human skull and monopoles were generated at individual contacts. A linear array ultrasound (US) transducer was coupled to the temporal window and focused toward the DBS electrode to induce AE signals proportional to the time-varying current densities. The AE signals using an injected current of 11 mA and focal pressures of 2.04 MPa were detected with SNRs between 7-16 dB, mean accuracy along the length of the electrode of 0.35 mm, radial separation of segmented contacts in a ring-triplet of 1.21 mm, mean monopole FWHMs of 3.54 mm, and a sensitivity of 0.283 $\mu V/mA/MPa$. Our results advocate AEI as a promising tool for providing non-invasive, high resolution feedback of the spread of current from a directional DBS electrode with potential roles in enhancing placement of the electrode and chronically monitoring the integrity of the stimulation.**

Keywords—steerable DBS, Parkinson's disease, ultrasound current density imaging, current source analysis, essential tremor

I. Introduction

Deep brain stimulation (DBS) can be an effective therapy for dyskinesia associated with Parkinson's disease and essential tremor with efficacy being heavily dependent on accurate electrode placement. New DBS electrodes employ multiple segmented contacts allowing for configurations that enable directional current steering to enhance the volumetric control of neuronal excitation [1]. However, existing clinical implementations gather minimal spatiotemporal feedback of the currents due to inadequate non-invasive, high resolution electrical imaging modalities. Acoustoelectric imaging (AEI) is a cutting-edge electrical mapping modality that might be well-suited for bridging this limitation. AEI uses the pressure from ultrasound (US) to modulate the tissue resistivity and produce a detectable fluctuation in a recordable voltage when there is a current source present in the tissue [2-5]. We recently demonstrated AEI of the currents from a clinical DBS electrode using a 1MHz single-element US transducer [6]. However, high resolution mapping of the contacts using a linear array focused through a common, clinically viable entrance point (temporal window) was not explored.

In this study we focus a high resolution (2.5 MHz, $\lambda = 0.6mm$) US linear array through the temporal window of a human skull to image the currents produced by a directional DBS electrode. We then assess the efficacy of AEI to visualize these currents. In particular, we compute the SNR of the AE signal, size of the monopoles, accuracy of mapping the monopoles to their stimulating contacts, radial separation of monopoles generated by each segmented contact within a ring-triplet, and the sensitivity of the system.

II. Methods

A. Acoustoelectric Imaging Theory

As sound travels through a medium, it modulates its density and, consequently, its initial resistivity, ρ, proportional to the pressure, P, of the propagating wave, scaled by an acoustoelectric interaction coefficient, K.

$$\Delta\rho = -K\rho\Delta P \quad (1)$$

Ignoring the lead field of the recording electrodes, the voltage, V, from the volume integration of current density source, J, in this medium will fluctuate proportional to changes in resistivity, as dictated by Ohm's law in (2),

$$V = \iiint J(\rho + \Delta\rho)\ dxdydz \quad (2)$$

By substituting (1) into (2) it becomes clear that a change in pressure can induce a change in voltage as written in (3).

$$V = \iiint J\rho(1 - K\Delta P)\ dxdydz \quad (3)$$

Hence, a pair of electrodes used to measure the voltage of a current source also detects this minor fluctuation in voltage due to the modulation by the pressure wave, occurring at the frequency of the pressure wave. By pulsing the US beam, the time-varying wave form of the current source can be sampled along the depth of the US focus. The US beam can also be refocused and scanned in the X,Y plane to image a volume encompassing a time-varying current source, providing samples of $J(x,y,z,t)$ in $\Delta P(x,y,z)$ sized chunks as indicated by the triple integral in (4).

$$\Delta V(x,y,z,t) \propto J(x,y,z,t)\Delta P(x,y,z) \quad (4)$$

Lastly, the recorded voltage can then be filtered into two bands, a low frequency band, V^{LF}, containing the power associated with the injected or physiological current, and a high frequency band around the frequency of the US wave, V^{AE}, which is the AE signal

$$V = V^{LF} + V^{AE} \quad (5)$$

B. *Acoustoelectric Imaging Bench-top Setup*

A DBS electrode (Abbott/St. Jude *Infinity model 6172ANS*) with 8 contacts enabled for current steering (Figure 1) was inserted into a conductive hydrogel brain phantom constructed inside a human skull (Figure 2). The hydrogel was composed of 10% porcine gelatin and 0.9% saline.

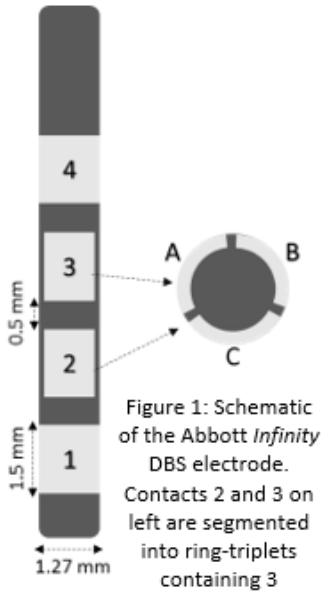

Figure 1: Schematic of the Abbott *Infinity* DBS electrode. Contacts 2 and 3 on left are segmented into ring-triplets containing 3 individual, identical contacts within each ring as shown on the right.

A function generator (33220A, Agilent, Santa Clara, CA, USA) produced time-varying current (3V, 200 Hz, 300 μs pulse) to create monopoles at individual contacts of the DBS electrode. A linear array transducer (2.5 MHz, 96 elements, Philips P4-1) was coupled to the temporal window of the human skull and focused near the DBS electrode. The US transducer was pulsed at 8kHz and at safe pressures [7] (2.04 MPa peak-to-peak at focus) using an open ultrasound system (Vantage 64 LE, Verasonics, Kirkland, WA, USA). First, the US beam was scanned across the length of the DBS electrode to provide 2D images of the time-varying current from a contact at each of the four rings. Next, the US transducer was rotated 90° and focused on a triplet of contacts, e.g. (2A, 2B, 2C), and scanned along the cross-section of the DBS electrode to image the individual monopoles from each of the three contacts.

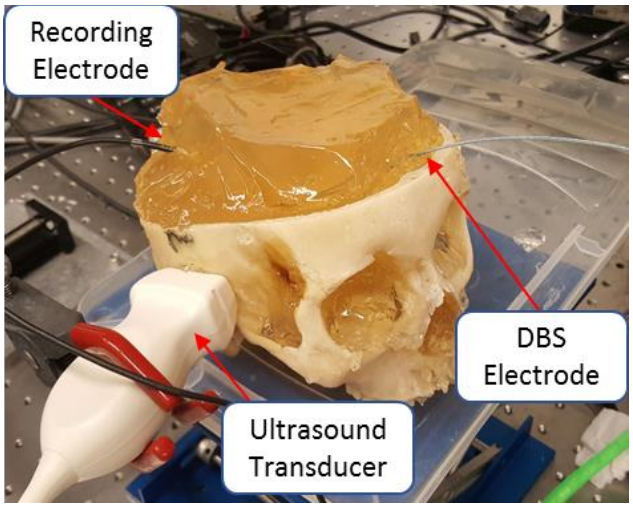

Figure 2: Photograph of the experimental setup indicating the locations of the DBS electrode, recording electrode and US transducer.

A single ended tungsten recording electrode (referenced to ground) was also inserted into the brain phantom to detect the AE signal. After analog detection, the AE signal was bandpass filtered (-3 dB cutoff at 0.2 and 5 MHz) with a gain of 40 dB before digitization at 20MHz on a 12-bit acquisition card. Additionally, the injected current was recorded across a 1-ohm resistor, low pass filtered (-3 dB at 10 kHz) and sampled at 20 kHz (NI PXI-6289, National Instruments, Austin, TX, USA) to provide the current waveform and amplitude. Pulse-echo US was also captured during one scan in each orientation to overlay the AE signal with the structure and orientation of the electrode.

III. Results and Discussion

With the US focused on a time-varying monopole, the AE signal was sampled by pulsing the US beam at 8kHz to determine the accuracy of AEI in detecting the 300μs pulse waveform produced by the DBS electrode. The injected current waveform was recorded and matched to the resulting AE signal (Figure 3). Given a 300μs pulse width and a time domain sampling rate of 125μs, only three samples were capturable per pulse of the DBS. Regardless, the relative amplitude of the AE signal matched very closely over time with amplitude of the injected current ($R^2 = 0.942$), which was also plotted against the amplitude of the corresponding AE signal over time to determine the sensitivity of the system: 0.283 $\mu V/mA/MPa$.

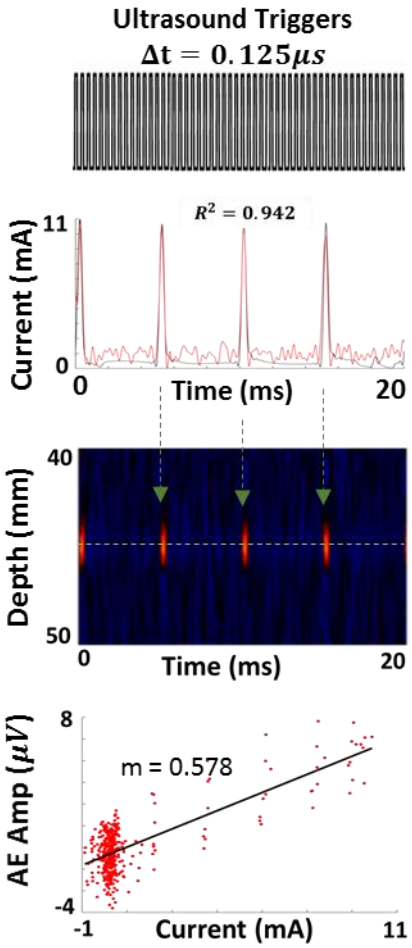

Figure 3: Timing schematic showing ultrasound pulses (top) in relation to the rectified injected current (black) with AE signal (red) taken at the depth along the green hashed line in the below M-Mode representation of the AE signal. The M-Mode AE image shows the unrectified signal at ± 6dB with positive (hot) and negative (cold) amplitudes. The bottom plot shows relation of AE signal amplitude referenced to injected current amplitude, where the slope gives the sensitivity of the system.

The US focus was then scanned through the temporal window along the length of the DBS electrode with spacing $\Delta x = 0.25\ mm$. Individual monopoles were generated at each of the contacts for each scan. Figure 4 shows the 2D images of the AE signals taken at peak current amplitudes overlaying the pulse echo of the DBS electrode. With the tip of the electrode considered as x=0, the distance between the centroid of each monopole was compared to the projected center of its stimulating contact knowing that there is 2mm separation between the center of adjacent contacts. The accuracy of each monopole's centroid mapped to the contact center using this method was 0.35 ± 0.11 mm. Additionally, the lateral FWHM of the monopoles was measured to be 3.54 ± 0.29mm.

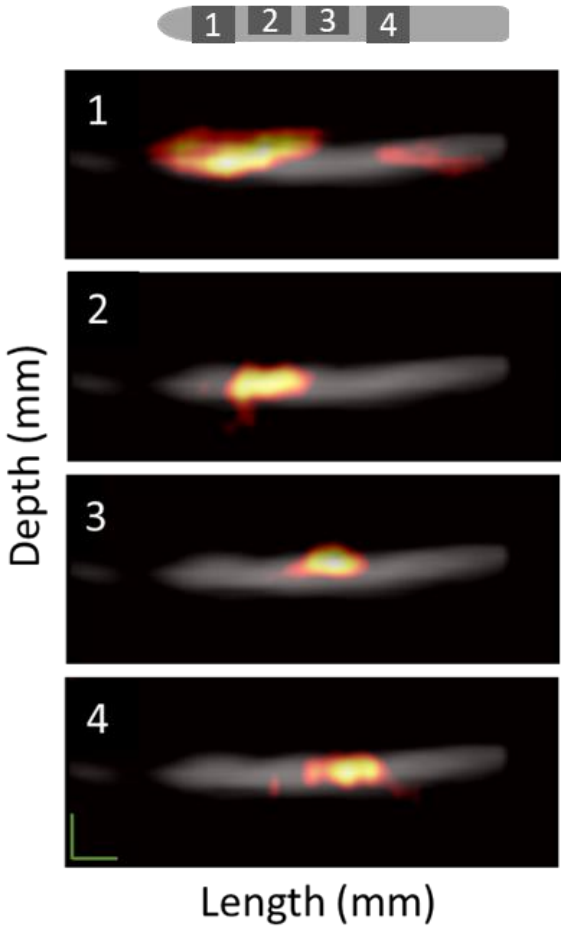

Figure 4: Longitudinal 2D transcranial AEI of the stimulated contact (hot) at peak current superimposed on the B-Mode pulse echo image of the DBS electrode (gray). Green bars on the bottom left image indicate 2mm in each direction. The cartoon at the top indicates the presumed length of the DBS electrode (with contact locations) based on the pulse echo image.

In our final experiment, the US probe was rotated 90° while maintaining focus through the temporal window to image along the cross-section of the DBS electrode. With the US beam focused toward one of the segmented triplets of contacts within one ring, e.g. 2A, 2B, 2C, individual monopoles were again generated by these contacts as the beam was steered along the cross-section of the DBS electrode to provide 2D images (Figure 5). Radial separation of the centroids from the monopoles was calculated to determine the feasibility of resolving between the three adjacent contacts within a single ring. The mean radial separation between contacts was calculated to be 1.21 ± 0.34 mm. This can be compared to the actual radial separations between contacts of 1.11 mm in each ring-triplet. Due to the distorted pulse echo captured during this orientation, absolute accuracy of the monopoles was not calculated. However, given the large separations, it was possible to match the stimulating contacts to the monopoles in the AE images to determine rotation of the DBS electrode despite the ineffective pulse echo.

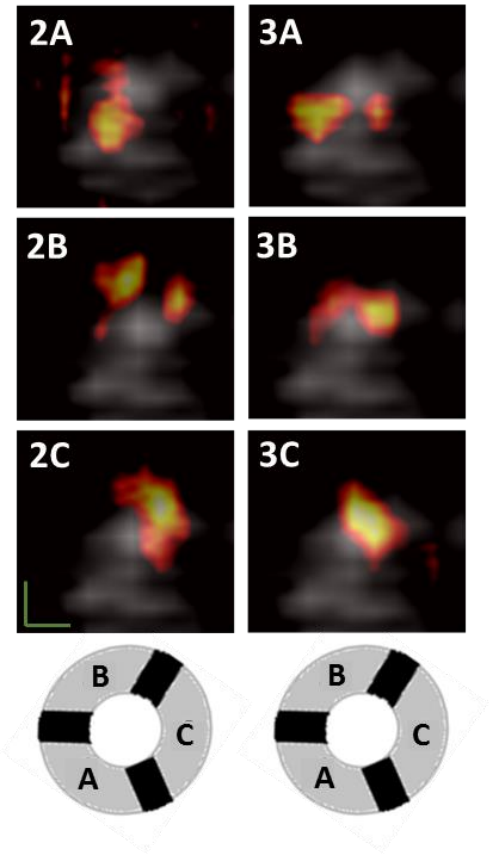

Figure 5: *Cross-sectional 2D transcranial AEI of the stimulated contact (hot) at peak current superimposed on the B-Mode pulse echo image of the DBS electrode (gray). Green bars on the bottom left image indicates 2mm in each direction. The donuts at the bottom depict the known orientation of the contacts.*

IV. Conclusions

Using a high spatial resolution ($\lambda = 0.6mm$) linear US array, clinically relevant currents (3V, 300μs pulse) from a DBS electrode were imaged with SNRs ranging from 7-16 dB. Monopoles generated by select contacts along the length of the DBS electrode could be matched to their stimulating contact with a mean accuracy of 0.35 mm. Moreover, a mean radial separation between individual contacts within a segmented ring-triplet of 1.21 mm is highly suggestive of accurate stimulating contact determination within each segmented ring, further highlighting the accuracy and resolution of AEI. A sensitivity of 0.283 $\mu V/mA/MPa$ combined with the SNRs achieved here indicates that current amplitudes less than 2 mA should be detectable while maintaining safe US pressures. Lastly, the time waveform of the injected current was accurately sampled with AEI ($R^2 = 0.942$), demonstrating the feasibility of detecting the brief stimulating pulses often used in DBS. Together, our results advocate AEI as a promising tool for providing non-invasive, high resolution feedback of the electrical currents generated during DBS, and due to its high accuracy, it may complement or potentially supersede other modalities for guiding placement of the device during surgery.

Acknowledgments

NIH NINDS R24MH109060
NIH Training Grant T32EB000809
NIH Training Grant T32HL007955
NIH Training Grant R25HD080811
University of Arizona Willed Body program for the human skull
Center for Gamma Ray Imaging for use of their 3D printer
Abbott for the DBS electrode used in the experiments

References

[1] Steigerwald, F., C. Matthies, and J. Volkmann, *Directional Deep Brain Stimulation.* Neurotherapeutics, 2019. **16**(1): p. 100-104.J. Clerk Maxwell, A Treatise on Electricity and Magnetism, 3rd ed., vol. 2. Oxford: Clarendon, 1892, pp.68–73.

[2] Jossinet, J., B. Lavandier, and D. Cathignol, *The phenomenology of acousto-electric interaction signals in aqueous solutions of electrolytes.* Ultrasonics, 1998.K. Elissa, "Title of paper if known," unpublished.

[3] Olafsson, R., et al., *Ultrasound current source density imaging.* IEEE Trans Biomed Eng, 2008. **55**(7): p. 1840-8.

[4] Berthon, B., et al., *An integrated and highly sensitive ultrafast acoustoelectric imaging system for biomedical applications.* Phys Med Biol, 2017. **62**(14): p. 5808-5822.M. Young, The Technical Writer's Handbook. Mill Valley, CA: University Science, 1989.

[5] Wang, Z., et al., Complementary Detection of Multiple Electrical Sources in Tissue Using Acoustoelectric Effects. Ultrasound Med Biol, 2016. **42**(9): p. 2323-33.

[6] Preston, C., W.S. Kasoff, and R.S. Witte, *Selective Mapping of Deep Brain Stimulation Lead Currents Using Acoustoelectric Imaging.* Ultrasound Med Biol, 2018.

[7] Harris G, P.R., Guidance for FDA and Industry Staff Information for Manufactureres Seeking Marketing Clearance of Diagnostic Ultrasound Systems and Transducers. 2008.